The British Journal of Radiology

Prognostication of overall survival in patients with brain metastases using diffusion tensor imaging and dynamic susceptibility contrast-enhanced MRI

--Manuscript Draft--

Manuscript Number:	BJR-D-22-00516R1
Full Title:	Prognostication of overall survival in patients with brain metastases using diffusion tensor imaging and dynamic susceptibility contrast-enhanced MRI
Short Title:	Prognostic value of DTI and DSC in predicting OS in brain metastases
Article Type:	Full Paper
Corresponding Author:	Suyash Mohan, M.D., P.D.C.C. University of Pennsylvania Philadelphia, PA UNITED STATES
Corresponding Author Secondary Information:	
Corresponding Author's Institution:	University of Pennsylvania
Corresponding Author's Secondary Institution:	
First Author:	Laiz Laura de Godoy
First Author Secondary Information:	
Order of Authors:	Laiz Laura de Godoy
	Yin Jie Chen
	Sanjeev Chawla
	Angela N Viaene
	Sumei Wang
	Laurie A Loevner
	Michelle Alonso-Basanta
	Harish Poptani
	Suyash Mohan, M.D., P.D.C.C.
Order of Authors Secondary Information:	
Abstract:	Objectives: To investigate the prognostic utility of DTI and DSC-PWI perfusion-derived parameters in brain metastases patients. Methods: Retrospective analyses of DTI-derived parameters (MD, FA, CL, CP, and CS) and DSC-perfusion PWI-derived rCBV max from 101 patients diagnosed with brain metastases prior to treatment were performed. Using semi-automated segmentation, DTI metrics and rCBV max were quantified from enhancing areas of the dominant metastatic lesion. For each metric, patients were classified as short and long-term survivors based on analysis of the best coefficient for each parameter and percentile to separate the groups. Kaplan-Meier analysis was used to compare mOS between these groups. Multivariate survival analysis was subsequently conducted. A correlative histopathologic analysis was performed in a subcohort (n=10) with DTI metrics and rCBV max on opposite ends of the spectrum. Results: Significant differences in mOS were observed for MD min ($p<0.05$), FA ($p<0.01$), CL ($p<0.05$), and CP ($p<0.01$) and trend towards significance for rCBV max ($p=0.07$) between the two risk group, in the univariate analysis. On multivariate analysis, the best predictive survival model was comprised of MD min ($p=0.05$), rCBV max ($p<0.05$), RPA ($p<0.0001$), and number of lesions ($p=0.07$). On histopathology, metastatic tumors showed significant differences in the amount of stroma depending on the combination of DTI metrics and rCBVmax values. Patients with high stromal content demonstrated poorer mOS.

	Conclusion: Pretreatment DTI-derived parameters, notably MD min , and rCBVmax, are promising imaging markers for prognostication of OS in patients with brain metastases. Stromal cellularity may be a contributing factor to these differences. Advances in knowledge: The correlation of DTI-derived metrics and perfusion MRI with patient outcomes has not been investigated in patients with treatment naïve brain metastasis. DTI and DSC-PWI can aid in therapeutic decision-making by providing additional clinical guidance.

Itemised List of Revisions - please do not include author details on this file

August 21, 2022

Dr. Mahmud Mossa-Basha
Senior Editor, *British Journal of Radiology (BJR)*

Ref: Manuscript Revision

Manuscript ID: BJR-D-22-00516. "Prognostication of overall survival in patients with brain metastases using diffusion tensor imaging and dynamic susceptibility contrast-enhanced MRI"

Dear Dr. Mossa-Basha and reviewers of BJR,

We would like to thank you for reviewing our manuscript entitled ***"Prognostication of overall survival in patients with brain metastases using diffusion tensor imaging and dynamic susceptibility contrast-enhanced MRI."*** We have made the requested changes to the manuscript addressing all issues brought up by the reviewers. We believe that the manuscript is now significantly improved as a result of the provided feedback. Enclosed is our point-by-point response to reviewers' comments.

We sincerely hope that this extensively revised manuscript will now be acceptable for publication in *BJR*.

POINT BY POINT RESPONSE TO REVIEWERS

We thank the reviewer for the careful review of our manuscript. We acknowledge that all of your feedback, both negative and positive, have been extremely helpful in the overall improvement of the paper. All sentences or words added to the text are highlighted in BLUE. Words removed from the text are highlighted in YELLOW.

Reviewer 1

The authors investigate the prognostic utility of DTI and DSC MRI perfusion-derived parameters in brain metastases patient, and Pretreatment DTI-derived parameters are promising imaging markers for prognostication of OS in patients with brain metastases. The authors work has merit and the manuscript is well written. The aims of the work are clear and sound interesting.

Response: The authors appreciate the reviewer's positive comments. Please find below our responses that address the other concerns:

1) Please, add the interobserver agreement studies for the DTI parameters and CBV measurement

Response: Thank you, for this comment. We would like to clarify that since only one co-author processed the DTI metrics and DSC-MRI-derived CBV values for the entire dataset using an automated approach, the interobserver agreement is not applicable.

2) DSC: How long was the sequence? How many dynamics?

Response: The acquisition time of the DSC sequence was 3 minutes 10 seconds and had 45 dynamics *("Forty-five sequential measurements were acquired for each section").* Both details have now been included in the '**Dynamic Susceptibility Contrast-Perfusion Weighted Imaging'** section (page 6).

3) The authors do not subanalyse their sample taking into account the primary cancer and I think this is very important for the final conclusions they expose.
4) The location, size, and number of tumors should be taken into account when differentiating the correlation between different parameters and prognosis.

Response: We appreciate the reviewer's suggestion. We have analyzed the data based on the primary tumor site and the number of brain metastasis as the reviewer indicated. The mOS using tumor primary site (lung, breast, melanoma, kidney, colon, or other) was not significantly different (log-rank $p>0.05$), and the number of brain metastasis showed a trend towards significance (log-rank $p=0.09$), as independent predictors in univariate analysis. This information is included in the Methods ("**Final Data and Statistical Analysis";** page 8) and Results section (**"Survival analysis";** page 10). Subsequently, we performed cox proportion hazard model combining the statistically significant imaging and clinical independent predictive parameters (MD_{min}, FA Q25, CL Q25, CP Q25, RPA, and GPA) and parameters with trends towards significance in OS, such as $rCBV_{max}$ ($p=0.07$) and number of brain metastasis ($p=0.09$). We found that the best predictive model was obtained by a combination of MD_{min} ($p=0.05$), $rCBV_{max}$ ($p<0.05$), RPA ($p<0.0001$), and number of metastatic brain lesions ($p=0.07$). Primary tumor type did not achieve statistical significance in multivariate analysis ($p>0.05$), and the number of lesions showed a borderline significant p-value ($p=0.07$). We have reinforced the importance of MD_{min} and $rCBV_{max}$ as imaging parameters in a multivariate analysis to predict OS and found RPA and number of lesions as possible clinical confounding factors. The multivariate analysis is included in the Abstract, Methods ("**Final Data and Statistical Analysis;** pages 8/9**),** Results **("Determination of the best predictive survival model";** page 10/11**),** and through the Discussion section.

5) And some minor comments:
Check terminology regarding DSC- MRI. Could it be better referred as DSC-PWI (Dynamic Susceptibility Contrast-Perfusion Weighted Imaging)?

Response: Thank you for noticing it. We have changed the terminology *"DSC-MRI"* to *"DSC-PWI"* throughout the text.

Reviewer 2

In this manuscript, the authors investigated that the prognostic utility of DTI and DSC MRI perfusion-derived parameters in brain metastases patients. The authors concluded that Pretreatment DTI-derived parameters are promising imaging markers for prognostication of OS in patients with brain metastases. It is an interesting topic. The manuscript was well-organized and well-written.

Response: The authors appreciate the reviewer's favorable comments. Please find below our responses that address the reviewer's other concerns:

Material and Methods:

1) As for the subjects' age, was it normal-distributed? If so, please use mean age ± SD, if not, please use median (range).

Response: It was normal distributed: mean age = 59 years, SD ± 12 years. This information is now provided in the **Patient Population** section of the revised manuscript (page 5).

2) The acquisition time for the DTI and T1 GRE sequences should be provided, as well as the imaging range, imaging plane for each sequence.

Response: We have included the acquisition time and imaging plane for each sequence in the **MR Imaging Data Acquisition** section (pages 6 and 7): DTI: 8 minutes/axial plane. DSC-PWI: 3 mins 10 seconds/ axial plane. T1-weighted 3D MPRAGE postcontrast: 3 mins 10 seconds/ axial plane. FLAIR: 3 minutes 10 seconds/axial plane.

3) Directional diffusivity metrics, including RD and AD, have been used to improve the characterization of the WM microstructure and to maximize specificity. Why are AD and RD values not measured?

Response: We agree with the reviewer that AD and RD can provide additional information about tissue parameters. However, we would like to point out that these parameters provide

similar information that can be obtained by CL and CP, which have already been included in the analysis. As we have shown multi-parametric analysis of the DSC and DTI can provide a better estimation of the median overall survival, and since these parameters already include CL and CP, we do not believe doing a separate/additional analysis of AD and RD will add anything new to the manuscript. As such, we have not made any changes to the manuscript in response to this comment.

4) Discussion

Although not statistically significant, the mechanism of the effect of rCBVmax on overall survival prognosis has not been clearly explained.

Response: $rCBV_{max}$ showed a trend towards significance in univariate analysis ($p=0.07$). However, it was in fact statistically significant ($p<0.05$) in the cox proportion hazard regression analysis. We have addressed and reinforced the possible mechanism of rCBV in overall survival of brain metastasis patients in the 4/5th paragraphs of the Discussion section (page 14). Our results and prior papers using MRI-based perfusion parameters in extracranial cancers (Chawla, S, et al, AJNR, 2018; Chawla, S, et al, AJNR, 2011; Lichtor, T, et al, Books on Demand, 2015; Ohno Y, et al, J Magn Reson Imaging, 2005) support the notion that tumors with relatively higher blood flow/volume are associated with increased oxygenation levels resulting in better access to chemotherapeutic drugs and radiosensitivity and are thereby associated with improved survival outcomes. Moreover, according to a prior histopathological study (Spanberger T, et al, *Clin Exp Metastasis*, 2013), small peritumoral edema around brain metastasis was correlated with low microvascular density and neoangiogenic vascularization and was more likely to show brain-invasive growth than tumors with large edema. Therefore, rCBV as a measure of angiogenic activity may indirectly reflect tumor infiltration and predict overall survival.

Prognostication of overall survival in patients with brain metastases using diffusion tensor imaging and dynamic susceptibility contrast-enhanced MRI

Running head: Prognostic value of DTI and DSC in predicting OS in brain metastases

Type of manuscript: Full paper

Laiz L. de Godoy[1]; Yin Jie Chen[1], Sanjeev Chawla[1], Angela N. Viaene[2], Sumei Wang[1], Laurie A Loevner[1], Michelle Alonso-Basanta[3], Harish Poptani[4], Suyash Mohan[1]

Department of Radiology[1], Perelman School of Medicine at the University of Pennsylvania, Philadelphia, PA. Division of Anatomic Pathology[2], Children's Hospital of Philadelphia, Philadelphia, PA. Department of Radiation Oncology[3], Perelman School of Medicine at the University of Pennsylvania, Philadelphia, PA. Department of Molecular and Clinical Cancer Medicine[4], University of Liverpool, United Kingdom

Address Correspondence to:

Suyash Mohan, MD.

Associate Professor of Radiology and Neurosurgery

Department of Radiology

Perelman School of Medicine at the University of Pennsylvania

Philadelphia, PA, USA

Tel. 215-662-6865

Email: suyash.mohan@pennmedicine.upenn.edu

Disclosure statement:

The authors have no actual or potential conflicts of interest.

Funding:

No funding was received for this study.

Abstract

Objectives: To investigate the prognostic utility of DTI and DSC-PWI perfusion-derived parameters in brain metastases patients.

Methods: Retrospective analyses of DTI-derived parameters (MD, FA, CL, CP, and CS) and DSC-perfusion PWI-derived $rCBV_{max}$ from 101 patients diagnosed with brain metastases prior to treatment were performed. Using semi-automated segmentation, DTI metrics and $rCBV_{max}$ were quantified from enhancing areas of the dominant metastatic lesion. For each metric, patients were classified as short and long-term survivors based on analysis of the best coefficient for each parameter and percentile to separate the groups. Kaplan-Meier analysis was used to compare mOS between these groups. Multivariate survival analysis was subsequently conducted. A correlative histopathologic analysis was performed in a subcohort (n=10) with DTI metrics and $rCBV_{max}$ on opposite ends of the spectrum.

Results: Significant differences in mOS were observed for MD_{min} ($p<0.05$), FA ($p<0.01$), CL ($p<0.05$), and CP ($p<0.01$) and trend towards significance for $rCBV_{max}$ ($p=0.07$) between the two risk group, in the univariate analysis. On multivariate analysis, the best predictive survival model was comprised of MD_{min} ($p=0.05$), $rCBV_{max}$ ($p<0.05$), RPA ($p<0.0001$), and number of lesions ($p=0.07$). On histopathology, metastatic tumors showed significant differences in the amount of

stroma depending on the combination of DTI metrics and rCBVmax values. Patients with high stromal content demonstrated poorer mOS.

Conclusion: Pretreatment DTI-derived parameters, notably MD_{min}, and rCBVmax, are promising imaging markers for prognostication of OS in patients with brain metastases. Stromal cellularity may be a contributing factor to these differences.

Advances in knowledge: The correlation of DTI-derived metrics and perfusion MRI with patient outcomes has not been investigated in patients with treatment naïve brain metastasis. DTI and DSC-PWI can aid in therapeutic decision-making by providing additional clinical guidance.

Abbreviations:

CL- linear coefficient; CP- planar coefficient; CS- spherical coefficient; DSC - dynamic susceptibility contrast; DTI - diffusion tensor imaging; FA-fractional anisotropy; MD – mean diffusivity; MDmin – minimum mean diffusivity; MRI – magnetic resonance imaging; mOS – median overall survival; rCBVmax- maximum relative cerebral blood volume

Prognostication of overall survival in patients with brain metastases using diffusion tensor imaging and dynamic susceptibility contrast-enhanced MRI

Running head: Prognostic value of DTI and DSC in predicting OS in brain metastases

Type of manuscript: Full paper

Abstract

Objectives: To investigate the prognostic utility of DTI and DSC-PWI perfusion-derived parameters in brain metastases patients.

Methods: Retrospective analyses of DTI-derived parameters (MD, FA, CL, CP, and CS) and DSC-perfusion PWI-derived $rCBV_{max}$ from 101 patients diagnosed with brain metastases prior to treatment were performed. Using semi-automated segmentation, DTI metrics and $rCBV_{max}$ were quantified from enhancing areas of the dominant metastatic lesion. For each metric, patients were classified as short and long-term survivors based on analysis of the best coefficient for each parameter and percentile to separate the groups. Kaplan-Meier analysis was used to compare mOS between these groups. Multivariate survival analysis was subsequently conducted. A correlative histopathologic analysis was performed in a subcohort (n=10) with DTI metrics and $rCBV_{max}$ on opposite ends of the spectrum.

Results: Significant differences in mOS were observed for MD_{min} ($p<0.05$), FA ($p<0.01$), CL ($p<0.05$), and CP ($p<0.01$) and trend towards significance for $rCBV_{max}$ ($p=0.07$) between the two risk group, in the univariate analysis. On multivariate analysis, the best predictive survival model was comprised of MD_{min} ($p=0.05$), $rCBV_{max}$ ($p<0.05$), RPA ($p<0.0001$), and number of lesions ($p=0.07$). On histopathology, metastatic tumors showed significant differences in the amount of

stroma depending on the combination of DTI metrics and rCBVmax values. Patients with high stromal content demonstrated poorer mOS.

Conclusion: Pretreatment DTI-derived parameters, notably MD_{min}, and rCBVmax, are promising imaging markers for prognostication of OS in patients with brain metastases. Stromal cellularity may be a contributing factor to these differences.

Advances in knowledge: The correlation of DTI-derived metrics and perfusion MRI with patient outcomes has not been investigated in patients with treatment naïve brain metastasis. DTI and DSC-PWI can aid in therapeutic decision-making by providing additional clinical guidance.

Abbreviations:

CL- linear coefficient; CP- planar coefficient; CS- spherical coefficient; DSC-PWI - Dynamic Susceptibility Contrast-Perfusion Weighted Imaging; DTI - diffusion tensor imaging; FA- fractional anisotropy; MD – mean diffusivity; MDmin – minimum mean diffusivity; MRI – magnetic resonance imaging; mOS – median overall survival; rCBVmax- maximum relative cerebral blood volume.

Introduction

Brain metastases are the most frequent central nervous system tumors in adults, with increasing incidence due to improved access to diagnostic imaging methods and prolonged survival from primary neoplasms.[1–3] It is therefore essential to accurately prognosticate these patients for appropriate therapeutic decision-making. Several scoring systems have been proposed to predict the prognosis of brain metastases. The *recursive portioning analysis* (RPA) assesses the Karnofsky performance status (KPS), age, controlled primary tumor, and extracranial metastasis; the *graded prognostic assessment* (GPA) evaluates KPS, age, number of brain metastasis, and extracranial metastasis; and the *diagnosis-specific graded prognostic assessment* (DS-GPA) considers the same characteristic as GPA in addition to primary tumor histology.[4–6]

It has been reported that the higher the number of quantitative measurements assessed, the less subjective the scoring system is.[7–9] GPA includes the number of brain metastases, and RPA does not, and GPA is found to be more clinically useful, providing better treatment guidance.[10] Moreover, RPA was inefficient in patients with more than four metastases[11] and large variability in prognosis was observed within the intermediate RPA II class,[12] while a lack of power was indicated to be a limitation of the DS-GPA in predicting survival between histologic subtypes.[6] Growing evidence suggests that when the prognosis is unclear, clinicians require additional guidance to select appropriate treatment recommendations. Multiparametric MRI including diffusion tensor imaging (DTI) and dynamic susceptibility contrast-perfusion weighted imaging (DSC-PWI) provides metabolic and physiologic information complementing the morphologic information about metastasis number and location, thereby providing added value to be used as objective biomarkers for prognostication purposes.[13]

A recent study suggested that combination of apparent diffusion coefficient (ADC) with clinical prognostic markers improves the prognostication of patients with resected brain metastases.[14] However, ADC, which has the same physiologic significance as mean diffusivity (MD), provides only the information about the magnitude of water molecular motion. DTI is commonly used for brain imaging and provides additional information about the tensor orientation and shape, including fractional anisotropy (FA), linear anisotropy (CL), and planar anisotropy (CP).[15,16] Previous studies, including from our group, have demonstrated the utility of DTI metrics in differentiating solitary brain metastasis from glioblastomas,[17–19,20] as well as for prediction of overall survival in glioblastoma patients.[21] These studies indicate that FA, CL, and CP values provide additional information about tumor diffusion characteristics, which may also be helpful to noninvasively assess the microstructure of brain metastasis, strengthening the utility of a single metric 'ADC' to better separate risk groups.

Besides DTI, DSC-PWI derived cerebral blood volume (CBV) is a relevant and potent biomarker to assess tumor angiogenesis and microvasculature,[22,23] and has been demonstrated to be a valid biomarker to predict survival in patients with newly diagnosed glioblastoma – patients with increased relative CBV were associated with poorer outcomes.[24–26] On the contrary, in a previous histopathologic analysis, patients with brain metastases with high microvascular density and a neoangiogenic vascularization pattern had favorable survival times.[27] However, pretreatment perfusion characteristics of brain metastases are yet to show significant prediction of overall response.[13,28,29]

The combination of both DTI and DSC-PWI derived metrics provides additional information on the intratumoral heterogeneity and has been shown to improve prognostication in high-grade

gliomas.[30–33] Therefore, in the present study, we aimed to investigate the prognostic utility of DTI and DSC- PWI derived parameters in a relatively large cohort of patients with treatment naïve brain metastases. In order to validate the imaging findings, correlative histopathologic analysis measuring stromal component (desmoplastic reaction) was performed in a subset of patients.

Materials and Methods

Patient Population

This retrospective study was approved by the institutional review board (IRB) and was compliant with the Health Insurance Portability and Accountability Act. The inclusion criteria included a histologically confirmed diagnosis of brain metastasis and availability of conventional and advanced (DTI and DSC-PWI) MRI scans prior to any treatment for brain metastasis.

Based upon the inclusion criteria, 101 patients (mean age = 59, SD ± 12 years, 49 males/ 52 females) with solitary and multiple brain metastases (two, three, or more than three) were included. Primary cancer was lung (n=56), breast (n=15), and other (n=30). Six patients were excluded from the analysis of DSC- PWI due to the presence of susceptibility artifacts. Clinical data included tumor type, KPS, GPA, RPA, and overall survival, which was measured as the time interval from initial MRI diagnosis of brain metastasis until the date of death (n=82) or last known clinical encounter, if the patient was alive (n=19). The details of each patient's demographic, clinical, and diffusion and perfusion MRI-derived parameters are described in Supplementary Table 1.

MR Imaging Data Acquisition

Diffusion Tensor imaging

Axial DTI data were acquired using 30 noncollinear/noncoplanar directions with a single-shot spin-echo, echo-planar read-out sequence with parallel imaging by using generalized autocalibrating partially parallel acquisition (GRAPPA) and acceleration factor of 2. The sequence parameters were as follows: repetition time (TR) / echo time (TE) = 5,000/86ms, number of excitations (NEX) = 3, field of view (FOV) = 22 x 22cm^2, matrix size = 128 x 128, in-plane resolution = 1.72 x 1.72 mm^2; slice thickness = 3 mm; b = 0, 1000 s/mm^2; number of slices = 40; acquisition time 8 minutes.

Dynamic Susceptibility Contrast-Perfusion Weighted Imaging

For axial DSC- PWI, a bolus of gadobenate dimeglumine (Multi-Hance; Bracco Diagnostics, Princeton, New Jersey) was injected with a preloading dose of 0.07 mmol/kg, to reduce the effect of contrast agent leakage on CBV measurements. A T2*-weighted gradient-echo EPI was used during the second 0.07 mmol /kg bolus of contrast agent for the DSC- PWI. The injection rate was 5 ml/s for all patients and was immediately followed by a flush of saline (total of 20 ml at the same rate). The sequence parameters were as follows: TR/TE = 2000/45 ms; FOV = 22 x 22 cm^2; matrix size = 128 x 128; in-plane resolution = 1.72 x 1.72 mm^2; slice thickness = 3 mm; BW = 1346 Hz/pixel; flip angle = 90°; EPI factor = 128; echo spacing = 0.83; acquisition time 3 minute and 10 seconds. Forty-five sequential measurements were acquired for each section. After the preloading dose of the contrast agent, routine sequences were also obtained, including axial T1-weighted 3D MPRAGE postcontrast (TR/TE/TI 1760/3.1/950 ms; 192 x 256 matrix size; 1-mm section thickness; acquisition time 3 minutes and 10 seconds) and axial FLAIR

(TR/TE/TI 9420/141/2500 ms; 3-mm section thickness; acquisition time 3 minutes and 10 seconds).

Image Processing and Data Analysis

The motion and eddy current correction modules were applied to raw DTI data using in-house developed software (IDL; ITT Visual Information Solutions, Boulder, Colorado). Pixel-wise MD, FA, CL, CP, and spherical coefficient (CS) maps were computed by using the methods described earlier.[34,35] Leakage-corrected CBV maps were generated by performing gamma-variate curve fitting from DSC-PWI data using NordicICE software (NordicNeuroLab, Bergen, Norway).

The DTI derived maps, CBV maps, and T2-FLAIR images were resliced and co-registered to contrast-enhanced T1-weighted images. A semiautomatic approach was used to segment the contrast-enhancing regions of the dominant metastatic lesion by using a signal intensity-based thresholding method as defined previously.[34,35]

Tissue-Based Analysis

Representative histologic sections stained with hematoxylin-eosin and Masson's Trichrome were used to assess the stromal component (desmoplastic reaction) within the tumor by a board-certified neuropathologist (A.N.V.). The staining procedure for Masson's Trichrome included: slides were deparaffinized and hydrated, thereafter placed in Bouin's fixative for 1 hour in 60˚ C oven, washed in running tap water for 5 minutes, rinsed in deionized water, and stained in Weigert's Iron Hematoxylin for 10 minutes. Subsequently, slides were washed in running tap water for 10 minutes, rinsed in deionized water, stained in Beibrich Scarlet- Acid Fuchsin

solution for 15 minutes, and rinsed in deionized water, stained in Phosphotungstic acid for 2 minutes. Finally, the slides were stained in Aniline Blue solution for 1 to 5 minutes, rinsed in 1% acetic acid, dehydrated and coverslipped. The amount of tumor stroma was qualitatively assessed as low (scant to little), moderate, and high (stroma comprising a noticeable proportion of the overall tumor volume).

Final Data and Statistical Analysis

DTI metrics and DSC-PWI derived CBV values were quantified from enhancing areas of dominant metastasis segmented semi-automatically, as described above. We used continuous values and various breakdowns in terms of coefficients (Q10, Q25, Q50, Q75, and Q90) for each parameter and percentiles (25th, 50th, and 75th percentile) to separate the patients into two risk groups (short and long-term survivors) in a univariate analysis. The best combination for each parameter from preliminary results was as follows, MD: the lower 10th percentile MD values (Q10) reported as minimum MD (MD_{min}) and subsequently separating the risk groups above and below the median (50th percentile) of the MD_{min}. FA/CL/CP/CS: the lower 25th percentile FA/CL/CP/CS values (Q25) and subsequently separated the risk groups above and below the first quartile (25th percentile) of the FA/CL/CP/CS Q25. rCBV: the top 90th percentile rCBV values (Q90) reported as $rCBV_{max}$ and subsequently separated the risk groups above and below the third quartile (75th percentile) of the $rCBV_{max}$. Kaplan-Meier survival curve plots and log-rank tests were used to compare the survival rates using the aforementioned imaging parameters (MD_{min}, FA Q25, CL Q25, CP Q25, CS Q25, and $rCBV_{max}$), as well as clinical variables (number of brain metastasis and site of primary tumor), and clinical scoring systems (GPA and RPA classes) as stratification factors. Subsequently, clinical and imaging variables that demonstrated significant predictive values and trends towards significance from univariate

survival analyses were incorporated into multivariate survival analysis using the Cox regression hazard model with backward conditional method. A probabilistic (p) value of less than 0.05 was considered significant. All statistical analyses were performed using a statistical package, SPSS for Windows (v. 18.0; Chicago, IL).

Additionally, a correlative histopathologic analysis was performed in a subset of patients on the opposite ends of the spectrum of DTI metrics and DSC-PWI derived $rCBV_{max}$. The DTI metrics were used as a surrogate marker of tumor cellularity and microarchitectural organization[13] and $rCBV_{max}$ for tumor angiogenesis and neovascularization.[27] Group 1 (n=6; Supplementary table 1: patients 12, 31, 66, 84, 87, and 94) was selected to represent the best combination of the lowest values of MD_{min} (impaired mobility of water; high cellularity) and the highest values of FA Q25 and CP Q25 (increased anisotropy; high organization of the tumor microarchitecture), and the lowest values of $rCBV_{max}$ (reduced angiogenesis; poor vascularity). Group 2 (n=4, Supplementary table 1: patients 13, 34, 77, and 81) was selected to have the best combination of the highest values of MD_{min} (facilitated mobility of water; low cellularity) and the lowest values of FA Q25 and CP Q25 (decreased anisotropy; poor organization of the tumor microarchitecture), and the highest values of $rCBV_{max}$ (elevated angiogenesis; increased vascularity). Of note, similar to the main cohort, this subcohort of patients also had metastatic tumors from a variety of primary sites (six lung adenocarcinomas, one breast adenocarcinoma, one colorectal adenocarcinoma, one high-grade neuroendocrine carcinoma of lung origin, and one sarcoma of lung origin).

Results

Survival analysis

The Median KPS score was 80, and the median overall survival (mOS) for all patients was 301 days. In univariate analysis, survival differences by GPA class was significant (log-rank $p<0.001$. Class 1: 339.35 +/-128.79 days; Class 2: 682.64+/-100.49 days; Class 3: 1519.86 days; and Class 4: 1553.67 +/-425.63 days) and also for RPA class (log-rank $p<0.001$. Class 1: 1533.13 +/- 238.61 days; Class 2: 505.25 +/-72.71 days; Class 3: 123.75 +/-30.09 days), indicating a valid cohort. The mOS using tumor primary site (lung, breast, melanoma, kidney, colon, or other) was not significantly different (log-rank $p>0.05$), and the number of brain metastasis showed a trend towards significance (log-rank $p=0.09$), as independent predictors in univariate analysis.

Determination of long and short-term survivors using MRI data

Kaplan-Meier analyses revealed significant differences in mOS for MD_{min} (log-rank $p<0.05$), FA Q25 (log-rank $p<0.01$), CL Q25 (log-rank $p<0.05$), and CP Q25 (log-rank $p<0.01$), and trend towards significance for $rCBV_{max}$ (log-rank $p=0.07$). However, CS Q25 (log-rank $p>0.05$) did not predict survival (Figures 1 and 2 and Table 1).

Determination of the best predictive survival model

When statistically significant imaging and clinical independent prognostication parameters (MD_{min}, FA Q25, CL Q25, CP Q25, RPA, and GPA) and parameters with trends towards significance, such as $rCBV_{max}$ (log-rank $p=0.07$) and number of metastatic brain lesions (log-rank $p=0.09$), from univariate analyses were incorporated into Cox proportion hazard regression test, the best predictive survival model was obtained, which consisted of a combination of MD_{min}

(p=0.05), $rCBV_{max}$ (p<0.05), RPA (p<0.0001), and number of brain metastasis (p=0.07) in determining the OS.

Tissue-Based Analysis

Metastatic tumors showed an overall higher interstitial connective tissue (stromal component) in group 1 (n=6, mOS 83.33 +/-12.41 days) as compared to group 2 (n=4, mOS 1858.00 +/-707.81 days). The lowest values of MD_{min} and $rCBV_{max,}$ along with the highest values of FA Q25 and CP Q25 (group 1) significantly correlated with elevated stromal content and worse mOS (Figure 3). On the other hand, the highest values of MD_{min} and $rCBV_{max,}$ along with the lowest values of FA Q25 and CP Q25 (group 2) correlated with lower stromal content and better mOS (Figure 4). A quantitative measurement of the stromal component was not performed due to large variability across the slides. Thus, a qualitative assessment of low, moderate and high component was used instead. Assessment of the stromal component was facilitated by Masson's Trichrome stained sections (blue staining). These findings were consistent within the two groups regardless of tumor site of primary origin.

Discussion

The prognostic value of ADC is well-known for extracranial cancers in predicting survival, response to therapy, and even propensity to form brain metastasis.[36,37] Primary CNS tumors with low ADC values have also been associated with worse outcomes.[38–40] Recently, ADC incorporated with standard clinical parameters has shown to improve the prediction of overall survival in patients with surgically resected brain metastasis.[14] In this study, the MD_{min}, FA Q25, CL Q25, CP 25, and CBV_{max} as independent measures separated risk groups in short and long-term survivors, and in a multivariate analysis, the combination of MD_{min}, $rCBV_{max}$, RPA, and the

number of brain metastasis was the best predictive survival model, reinforcing the importance of MD_{min} and $rCBV_{max}$ as imaging parameters to predict OS and a possible confounding effect of RPA and the number of metastatic lesions. In addition, we demonstrated a correlation between the amount of desmoplastic reaction and mOS, substantiating the DTI metrics and $rCBV_{max}$ values.

The correlation of DTI-derived parameters and perfusion with patient outcomes has not been investigated in treatment naïve brain metastasis. However, a few studies reported the importance of ADC values in predicting survival in preoperative brain metastasis.[41,42] These studies reported aggressive tumor behavior in patients with low ADC values. In accordance with these studies, we also observed lower mOS in patients with MD_{min} below the median (similar physiological significance of ADC), and the MD_{min} remained statistically significant in multivariate analysis, supporting its prognostication value. However, other studies,[17–19] including from our group,[20] have demonstrated that the application of more gradient directions (DTI) can provide further tissue characterization and potentially be utilized for prognostication. We, therefore, evaluated several DTI parameters to noninvasively assess the tumor microarchitecture, demonstrating poor mOS in patients with low MD_{min} (impaired mobility of water) and high FA Q25, CL Q25, and CP 25 values (increased anisotropy). In other words, patients with high cellularity and organization of the tumor microarchitecture comprised short-term survivors. On the other hand, patients with high MD_{min} (facilitated mobility of water) and low FA Q25, CL Q25, and CP 25 values (decreased anisotropy), that is, low cellularity and disorganization of the tumor microarchitecture, were represented by long-term survivors.

Histopathologic studies have identified dense stromal matrix in primary tumors characterized by increased collagen fibril stiffness and anisotropy, described as a desmoplastic reaction, corroborating tumor growth.[43,44] In preoperative brain metastasis, Berghoff *et al.* 2013[42] reported a significant correlation of prominent interstitial fibrosis with the semiquantitative DWI signal intensity, resembling the impaired mobility of water molecules in the intercellular space. By extending the quantitative assessment of multiple DTI parameters, we demonstrated higher stromal component in patients with overall worse survival prognosis, represented by the lowest MD_{min} values and the highest values of FA Q25 and CP Q25. In contrast, patients with the highest MD_{min} values and the lowest FA Q25 and CP Q25 values presented with low cellular stromal component and had better long-term survival. These results from analyzed DTI metrics may reflect the tumor microarchitecture density and organization, reinforcing the importance of the interstitial space in the pathobiology of brain metastasis and the potential of quantitative DTI metrics to indirectly evaluate histopathological features.

The efficacy of chemoradiation therapy relies on the effective delivery of therapeutic agents and oxygen to the tumor cells. However, delivery of the drug and oxygen is often impeded by abnormal blood vessels and the presence of tumor hypoxia.[45] Using MRI-based perfusion parameters such as vascular transfer constant ($K^{trans,}$ a measure of tumor blood flow and vascular permeability), several previous studies[46–49] have reported that patients with extracranial cancers exhibiting elevated pretreatment K^{trans} harbor prolonged OS. In the present study, $rCBV_{max}$ was found to be a significant predictor in the determination of OS from Cox regression analysis, and brain metastasis patients with higher pretreatment $rCBV_{max}$ had longer mOS. Our results and those of earlier published reports support the notion that tumors with relatively higher blood flow/volume are associated with increased oxygenation levels resulting in better access to

chemotherapeutic drugs and radiosensitivity and thereby associated with improved survival outcomes.

The dense stromal matrix has also been correlated with pancreatic ductal adenocarcinoma with deficient vasculature limiting the delivery of chemotherapy and resulting in resistance to systemic therapies.[50] Therapeutic targeting of stromal cells increases intratumoral perfusion and enhances therapeutic delivery. In the current study, the group of patients with the lowest values of $rCBV_{max}$ (reduced tumor angiogenesis) showed higher stromal component and dismal survival rates. According to a prior histopathological study,[27] small peritumoral edema around brain metastasis was correlated with low microvascular density and neoangiogenic vascularization and was more likely to show brain-invasive growth than tumors with large edema. Therefore, rCBV as a measure of angiogenic activity may indirectly reflect tumor infiltration and predict OS.

There is a growing body of evidence supporting that advanced MRI techniques could potentially be integrated into the widely validated prognostic models for brain metastases patients,[14] such as RPA or GPA scores, which can be improved with quantitative imaging metrics assessing the metabolic and physiologic information of the tumor. Our results suggest that the incorporation of $rCBV_{max}$ and MD_{min} could further enhance these prognostic markers, potentially contributing to therapeutic decision-making. For example, in future, brain metastases patients with a good prognosis can be offered more aggressive treatments, whereas, in patients with poor prognosis, optimal treatment focused on quality of life would be deemed more appropriate.

Despite promising findings, our study was also associated with certain limitations, including the retrospective study design. In addition, histological correlation was only performed on a limited

sample size. Furthermore, our data is from a single institution and could benefit from validation in a multi-institutional cohort, preferably in a larger prospective study.

Conclusion

In conclusion, we reported the prognostic value of DTI metrics and $rCBV_{max}$ in segregating long and short-term survivors with brain metastasis and their correlation with tissue-based stromal features. Additionally, we reinforced the importance of MD_{min} and $rCBV_{max}$ in a multivariate analysis. Further validation in larger prospective studies in a multi-institutional setting may substantiate the incorporation of advanced imaging techniques into established risk stratification models.

References

1. Soffietti R, Rudā R, Mutani R. Management of brain metastases. *J Neurol* 2002;249:1357–69.

2. Gavrilovic IT, Posner JB. Brain metastases: epidemiology and pathophysiology. *J Neurooncol* 2005;75:5–14.

3. Fox BD, Cheung VJ, Patel AJ, et al. Epidemiology of metastatic brain tumors. *Neurosurg Clin N Am* 2011;22:1–6, v.

4. Sperduto PW, Berkey B, Gaspar LE, et al. A new prognostic index and comparison to three other indices for patients with brain metastases: an analysis of 1,960 patients in the RTOG database. *Int J Radiat Oncol Biol Phys* 2008;70:510–4.

5. Gaspar L, Scott C, Rotman M, et al. Recursive partitioning analysis (RPA) of prognostic factors in three radiation therapy oncology group (RTOG) brain metastases trials. *International Journal of Radiation Oncology*Biology*Physics* 1997;37:745–51.

6. Sperduto PW, Kased N, Roberge D, et al. Summary report on the graded prognostic assessment: an accurate and facile diagnosis-specific tool to estimate survival for patients with brain metastases. *J Clin Oncol* 2012;30:419–25.

7. Yamamoto M, Sato Y, Serizawa T, et al. Subclassification of recursive partitioning analysis Class II patients with brain metastases treated radiosurgically. *Int J Radiat Oncol Biol Phys* 2012;83:1399–405.

8. Serizawa T, Higuchi Y, Nagano O, et al. Testing different brain metastasis grading systems in stereotactic radiosurgery: Radiation Therapy Oncology Group's RPA, SIR, BSBM, GPA, and modified RPA. *J Neurosurg* 2012;117 Suppl:31–7.

9. Barnholtz-Sloan JS, Yu C, Sloan AE, et al. A nomogram for individualized estimation of survival among patients with brain metastasis. *Neuro Oncol* 2012;14:910–8.

10. Viani GA, Bernardes da Silva LG, Stefano EJ. Prognostic Indexes for Brain Metastases: Which Is the Most Powerful? *International Journal of Radiation Oncology*Biology*Physics* 2012;83:e325–30.

11. Nieder C, Andratschke N, Grosu AL, et al. Recursive partitioning analysis (RPA) class does not predict survival in patients with four or more brain metastases. *European Journal of Cancer* 2001;37:S341.

12. Estabrook NC, Lutz ST, Johnson CS, et al. Does Graded Prognostic Assessment outperform Recursive Partitioning Analysis in patients with moderate prognosis brain metastases? *CNS Oncology* 2016;5:69–76.

13. Pope WB. Brain metastases: neuroimaging. *Handb Clin Neurol* 2018;149:89–112.

14. Zakaria R, Chen YJ, Hughes DM, et al. Does the application of diffusion weighted imaging improve the prediction of survival in patients with resected brain metastases? A retrospective multicenter study. *Cancer Imaging* 2020;20:16.

15. Alexander AL, Hasan K, Kindlmann G, et al. A geometric analysis of diffusion tensor measurements of the human brain. *Magn Reson Med* 2000;44:283–91.

16. Westin C-F, Maier SE, Mamata H, et al. Processing and visualization for diffusion tensor MRI. *Med Image Anal* 2002;6:93–108.

17. Calli C, Kitis O, Yunten N, et al. Perfusion and diffusion MR imaging in enhancing malignant cerebral tumors. *Eur J Radiol* 2006;58:394–403.

18. Tsuchiya K, Fujikawa A, Nakajima M, et al. Differentiation between solitary brain metastasis and high-grade glioma by diffusion tensor imaging. *Br J Radiol* 2005;78:533–7.

19. Yamasaki F, Kurisu K, Satoh K, et al. Apparent diffusion coefficient of human brain tumors at MR imaging. *Radiology* 2005;235:985–91.

20. Wang S, Kim S, Chawla S, et al. Differentiation between Glioblastomas, Solitary Brain Metastases, and Primary Cerebral Lymphomas Using Diffusion Tensor and Dynamic Susceptibility Contrast-Enhanced MR Imaging. *American Journal of Neuroradiology* 2011;32:507–14.

21. Mohan S, Wang S, Coban G, et al. Detection of occult neoplastic infiltration in the corpus callosum and prediction of overall survival in patients with glioblastoma using diffusion tensor imaging. *Eur J Radiol* 2019;112:106–11.

22. Lacerda S, Law M. Magnetic resonance perfusion and permeability imaging in brain tumors. *Neuroimaging Clin N Am* 2009;19:527–57.

23. Thompson G, Mills SJ, Stivaros SM, et al. Imaging of brain tumors: perfusion/permeability. *Neuroimaging Clin N Am* 2010;20:337–53.

24. Romano A, Pasquini L, Di Napoli A, et al. Prediction of survival in patients affected by glioblastoma: histogram analysis of perfusion MRI. *J Neurooncol* 2018;139:455–60.

25. Law M, Young RJ, Babb JS, et al. Gliomas: Predicting Time to Progression or Survival with Cerebral Blood Volume Measurements at Dynamic Susceptibility-weighted Contrast-enhanced Perfusion MR Imaging. *Radiology* 2008;247:490–8.

26. Bag AK, Cezayirli PC, Davenport JJ, et al. Survival analysis in patients with newly diagnosed primary glioblastoma multiforme using pre- and post-treatment peritumoral perfusion imaging parameters. *J Neurooncol* 2014;120:361–70.

27. Spanberger T, Berghoff AS, Dinhof C, et al. Extent of peritumoral brain edema correlates with prognosis, tumoral growth pattern, HIF1a expression and angiogenic activity in patients with single brain metastases. *Clin Exp Metastasis* 2013;30:357–68.

28. Essig M, Waschkies M, Wenz F, et al. Assessment of Brain Metastases with Dynamic Susceptibility-weighted Contrast-enhanced MR Imaging: Initial Results. *Radiology* 2003;228:193–9.

29. Zakaria R, Das K, Bhojak M, et al. The role of magnetic resonance imaging in the management of brain metastases: diagnosis to prognosis. *Cancer Imaging* 2014;14:8.

30. Brancato V, Nuzzo S, Tramontano L, et al. Predicting Survival in Glioblastoma Patients Using Diffusion MR Imaging Metrics—A Systematic Review. *Cancers* 2020;12:2858.

31. Park JE, Kim HS, Jo Y, et al. Radiomics prognostication model in glioblastoma using diffusion- and perfusion-weighted MRI. *Scientific Reports* 2020;10.

32. Petrova L, Korfiatis P, Petr O, et al. Cerebral blood volume and apparent diffusion coefficient - Valuable predictors of non-response to bevacizumab treatment in patients with recurrent glioblastoma. *J Neurol Sci* 2019;405:116433.

33. Puig J, Sánchez-González J, Blasco G, et al. Intravoxel Incoherent Motion Metrics as Potential Biomarkers for Survival in Glioblastoma. *PLoS One* 2016;11:e0158887.

34. Wang S, Kim S, Chawla S, et al. Differentiation between glioblastomas and solitary brain metastases using diffusion tensor imaging. *Neuroimage* 2009;44:653–60.

35. Chawla S, Wang S, Mohan S, et al. Differentiation of brain infection from necrotic glioblastoma using combined analysis of diffusion and perfusion MRI. *J Magn Reson Imaging* 2019;49:184–94.

36. Nakajo M, Kajiya Y, Kaneko T, et al. FDG PET/CT and diffusion-weighted imaging for breast cancer: prognostic value of maximum standardized uptake values and apparent diffusion coefficient values of the primary lesion. *European Journal of Nuclear Medicine and Molecular Imaging* 2010;37:2011–20.

37. Ohno Y, Koyama H, Yoshikawa T, et al. Diffusion-Weighted MRI Versus 18F-FDG PET/CT: Performance as Predictors of Tumor Treatment Response and Patient Survival in Patients With Non–Small Cell Lung Cancer Receiving Chemoradiotherapy. *American Journal of Roentgenology* 2012;198:75–82.

38. Barajas RF Jr, Rubenstein JL, Chang JS, et al. Diffusion-weighted MR imaging derived apparent diffusion coefficient is predictive of clinical outcome in primary central nervous system lymphoma. *AJNR Am J Neuroradiol* 2010;31:60–6.

39. Wu C-C, Jain R, Radmanesh A, et al. Predicting Genotype and Survival in Glioma Using Standard Clinical MR Imaging Apparent Diffusion Coefficient Images: A Pilot Study from The Cancer Genome Atlas. *AJNR Am J Neuroradiol* 2018;39:1814–20.

40. Kim BS, Kim ST, Kim JH, et al. Apparent Diffusion Coefficient as a Predictive Biomarker for Survival in Patients with Treatment-Naive Glioblastoma Using Quantitative Multiparametric Magnetic Resonance Profiling. *World Neurosurgery* 2019;122:e812–20.

41. Zakaria R, Das K, Radon M, et al. Diffusion-weighted MRI characteristics of the cerebral metastasis to brain boundary predicts patient outcomes. *BMC Medical Imaging* 2014;14.

42. Berghoff AS, Spanberger T, Ilhan-Mutlu A, et al. Preoperative diffusion-weighted imaging of single brain metastases correlates with patient survival times. *PLoS One* 2013;8:e55464.

43. Koontongkaew S. The tumor microenvironment contribution to development, growth, invasion and metastasis of head and neck squamous cell carcinomas. *J Cancer* 2013;4:66–83.

44. Pham TT, Stait-Gardner T, Lee CS, et al. Correlation of ultra-high field MRI with histopathology for evaluation of rectal cancer heterogeneity. *Sci Rep* 2019;9:9311.

45. Vaupel P, Kallinowski F, Okunieff P. Blood flow, oxygen and nutrient supply, and metabolic microenvironment of human tumors: a review. *Cancer Res* 1989;49:6449–65.

46. Chawla S, Loevner LA, Kim SG, et al. Dynamic Contrast-Enhanced MRI-Derived Intracellular Water Lifetime (τ): A Prognostic Marker for Patients with Head and Neck Squamous Cell Carcinomas. *AJNR Am J Neuroradiol* 2018;39:138–44.

47. Chawla S, Kim S, Loevner LA, et al. Prediction of disease-free survival in patients with squamous cell carcinomas of the head and neck using dynamic contrast-enhanced MR imaging. *AJNR Am J Neuroradiol* 2011;32:778–84.

48. Lichtor T. *Molecular Considerations and Evolving Surgical Management Issues in the Treatment of Patients with a Brain Tumor*. BoD – Books on Demand; 2015.

49. Ohno Y, Nogami M, Higashino T, et al. Prognostic value of dynamic MR imaging for non-small-cell lung cancer patients after chemoradiotherapy. *J Magn Reson Imaging* 2005;21:775–83.

50. Neesse A, Michl P, Frese KK, et al. Stromal biology and therapy in pancreatic cancer. *Gut* 2011;60:861–8.

Figures' legends:

Figure 1: Kaplan Meier curves showing significantly higher overall survival (log-rank p=0.013) in patients with MD_{min} above 50^{th} percentile, significantly higher overall survival (log-rank p=0.009) in patients with FA Q25 below 25^{th} percentile, and significantly higher overall survival (log-rank p=0.009) in patients with CP Q25 below 25^{th} percentile.

Figure 2: Kaplan Meier curves showing non-significant differences in overall survival in terms of CS Q25 (log-rank p=0.384) and $rCBV_{max}$ (log-rank p=0.073).

Figure 3: 55-year-old female with metastatic adenocarcinoma of colorectal origin, prior to any treatment for brain metastasis, presenting with mOS of 62 days. (A) Contrast-enhanced T1-weighted image shows a heterogeneous enhancing lesion in the left inferior frontal lobe. (B) FLAIR images demonstrate surrounding vasogenic edema. (C) Decreased ADC (ADC_{min} = 0,000692) and (D) very high FA (FA Q25 = 0,12) values from the enhancing part. (E) DSC-PWI with low rCBV from the enhancing region of the tumor ($rCBV_{max}$ = 6.28; white arrows in E). (F) and (G) Pathology from surgical resection demonstrates high stromal component (blue staining, black arrows in G). H&E stain (F) and Masson's trichrome stain (G). Histological photos were taken at 100x magnification.

Figure 4: 45-year-old female with metastatic adenocarcinoma of breast, prior to any treatment for brain metastasis, presenting with mOS of 2859 days. (A) Contrast-enhanced T1-weighted image shows a ring enhancing lesion delimitating a central area of necrosis in the left temporal lobe. (B) FLAIR images demonstrate surrounding vasogenic edema. (C) Increased ADC (ADC_{min} = 0,000905) and (D) very low FA (FA Q25 = 0,057) values from the enhancing part. (E) DSC- PWI with elevated rCBV from the enhancing region of the tumor ($rCBV_{max}$ = 8.64, white arrows in E). (F) and (G) Pathology from surgical resection demonstrates a smaller stromal

component (blue staining, white arrows in G). H&E stain (F) and Masson's trichrome stain (G). Histological photos were taken at 100x magnification.

Table 1:

Title: Determination of long and short-term survivors using MRI data.

Supplementary Table1:

Title: Demographic, clinical, and diffusion and perfusion MRI-derived parameters.

Abbreviations: BM = brain metastasis; **KPS** = Karnofsky performance status; **GPA:** graded prognostic assessment. **RPA** = recursive portioning analysis; OS: overall survival. $\mathbf{MD_{min}}$: minimum mean diffusivity. **FA** = fractional anisotropy; **CP** = planar coefficien; **CS** = spherical coefficient. $\mathbf{rCBV_{max}}$ = maximum relative cerebral blood volume.

Prognostication of overall survival in patients with brain metastases using diffusion tensor imaging and dynamic susceptibility contrast-enhanced MRI

Running head: Prognostic value of DTI and DSC in predicting OS in brain metastases

Type of manuscript: Full paper

Abstract

Objectives: To investigate the prognostic utility of DTI and DSC-PWI MRI perfusion-derived parameters in brain metastases patients.

Methods: Retrospective analyses of DTI-derived parameters (MD, FA, CL, CP, and CS) and DSC-perfusion MRI PWI-derived $rCBV_{max}$ from 101 patients diagnosed with brain metastases prior to treatment were performed. Using semi-automated segmentation, DTI metrics and $rCBV_{max}$ were quantified from enhancing areas of the dominant metastatic lesion. For each metric, patients were classified as short and long-term survivors based on analysis of the best coefficient for each parameter and percentile to separate the groups. Kaplan-Meier analysis was used to compare mOS between these groups. Multivariate survival analysis was subsequently conducted. A correlative histopathologic analysis was performed in a subcohort (n=10) with DTI metrics and $rCBV_{max}$ on opposite ends of the spectrum.

Results: Significant differences in mOS were observed for MD_{min} ($p<0.05$), FA ($p<0.01$), CL ($p<0.05$), and CP ($p<0.01$) and trend towards significance for $rCBV_{max}$ ($p=0.07$) between the two risk group, in the univariate analysis. However, CS and rCBVmax did not demonstrate a significant difference in these groups ($p>0.05$). On multivariate analysis, the best predictive survival model was comprised of MD_{min} ($p=0.05$), $rCBV_{max}$ ($p<0.05$), RPA ($p<0.0001$), and number of lesions ($p=0.07$). On histopathology, metastatic tumors showed significant differences

in the amount of stroma depending on the combination of DTI metrics and rCBVmax values. Patients with high stromal content demonstrated poorer mOS.

Conclusion: Pretreatment DTI-derived parameters, notably MD_{min}, and rCBVmax, are promising imaging markers for prognostication of OS in patients with brain metastases. Stromal cellularity may be a contributing factor to these differences.

Advances in knowledge: The correlation of DTI-derived metrics and perfusion MRI with patient outcomes has not been investigated in patients with treatment naïve brain metastasis. DTI and DSC-PWI MRI can aid in therapeutic decision-making by providing additional clinical guidance.

Abbreviations:

CL- linear coefficient; CP- planar coefficient; CS- spherical coefficient; DSC-PWI - Dynamic Susceptibility Contrast-Perfusion Weighted Imaging; DTI - diffusion tensor imaging; FA- fractional anisotropy; MD – mean diffusivity; MDmin – minimum mean diffusivity; MRI – magnetic resonance imaging; mOS – median overall survival; rCBVmax- maximum relative cerebral blood volume

Introduction

Brain metastases are the most frequent central nervous system tumors in adults, with increasing incidence due to improved access to diagnostic imaging methods and prolonged survival from primary neoplasms.[1–3] It is therefore essential to accurately prognosticate these patients for appropriate therapeutic decision-making. Several scoring systems have been proposed to predict the prognosis of brain metastases. The *recursive portioning analysis* (RPA) assesses the Karnofsky performance status (KPS), age, controlled primary tumor, and extracranial metastasis; the *graded prognostic assessment* (GPA) evaluates KPS, age, number of brain metastasis, and extracranial metastasis; and the *diagnosis-specific graded prognostic assessment* (DS-GPA) considers the same characteristic as GPA in addition to primary tumor histology.[4–6]

It has been reported that the higher the number of quantitative measurements assessed, the less subjective the scoring system is.[7–9] GPA includes the number of brain metastases, and RPA does not, and GPA is found to be more clinically useful, providing better treatment guidance.[10] Moreover, RPA was inefficient in patients with more than four metastases[11] and large variability in prognosis was observed within the intermediate RPA II class,[12] while a lack of power was indicated to be a limitation of the DS-GPA in predicting survival between histologic subtypes.[6] Growing evidence suggests that when the prognosis is unclear, clinicians require additional guidance to select appropriate treatment recommendations. Multiparametric MRI including diffusion tensor imaging (DTI) and dynamic susceptibility contrast-perfusion weighted imaging (DSC-PWI) provides metabolic and physiologic information complementing the morphologic information about metastasis number and location, thereby providing added value to be used as objective biomarkers for prognostication purposes.[13]

A recent study suggested that combination of apparent diffusion coefficient (ADC) with clinical prognostic markers improves the prognostication of patients with resected brain metastases.[14] However, ADC, which has the same physiologic significance as mean diffusivity (MD), provides only the information about the magnitude of water molecular motion. DTI is commonly used for brain imaging and provides additional information about the tensor orientation and shape, including fractional anisotropy (FA), linear anisotropy (CL), and planar anisotropy (CP).[15,16] Previous studies, including from our group, have demonstrated the utility of DTI metrics in differentiating solitary brain metastasis from glioblastomas,[17–19,20] as well as for prediction of overall survival in glioblastoma patients.[21] These studies indicate that FA, CL, and CP values provide additional information about tumor diffusion characteristics, which may also be helpful to noninvasively assess the microstructure of brain metastasis, strengthening the utility of a single metric 'ADC' to better separate risk groups.

Besides DTI, DSC-PWI MRI derived cerebral blood volume (CBV) is a relevant and potent biomarker to assess tumor angiogenesis and microvasculature,[22,23] and has been demonstrated to be a valid biomarker to predict survival in patients with newly diagnosed glioblastoma – patients with increased relative CBV were associated with poorer outcomes.[24–26] On the contrary, in a previous histopathologic analysis, patients with brain metastases with high microvascular density and a neoangiogenic vascularization pattern had favorable survival times.[27] However, pretreatment perfusion characteristics of brain metastases are yet to show significant prediction of overall response.[13,28,29]

The combination of both DTI and DSC-PWI MR-derived metrics provides additional information on the intratumoral heterogeneity and has been shown to improve prognostication in

high-grade gliomas.[30–33] Therefore, in the present study, we aimed to investigate the prognostic utility of DTI and DSC- PWI MR derived parameters in a relatively large cohort of patients with treatment naïve brain metastases. In order to validate the imaging findings, correlative histopathologic analysis measuring stromal component (desmoplastic reaction) was performed in a subset of patients.

Materials and Methods

Patient Population

This retrospective study was approved by the institutional review board (IRB) and was compliant with the Health Insurance Portability and Accountability Act. The inclusion criteria included a histologically confirmed diagnosis of brain metastasis and availability of conventional and advanced (DTI and DSC-PWI) MRI scans prior to any treatment for brain metastasis.

Based upon the inclusion criteria, 101 patients (mean age = 59, SD ± 12 years, 49 males/ 52 females) with solitary and multiple brain metastases (two, three, or more than three) were included. Primary cancer was lung (n=56), breast (n=15), and other (n=30). Six patients were excluded from the analysis of DSC- PWI MR due to the presence of susceptibility artifacts. Clinical data included tumor type, KPS, GPA, RPA, and overall survival, which was measured as the time interval from initial MRI diagnosis of brain metastasis until the date of death (n=82) or last known clinical encounter, if the patient was alive (n=19). The details of each patient's demographic, clinical, and diffusion and perfusion MRI-derived parameters are described in Supplementary Table 1.

MR Imaging Data Acquisition

Diffusion Tensor imaging

Axial DTI data were acquired using 30 noncollinear/noncoplanar directions with a single-shot spin-echo, echo-planar read-out sequence with parallel imaging by using generalized autocalibrating partially parallel acquisition (GRAPPA) and acceleration factor of 2. The sequence parameters were as follows: repetition time (TR) / echo time (TE) = 5,000/86ms, number of excitations (NEX) = 3, field of view (FOV) = 22 x 22cm^2, matrix size = 128 x 128, in-plane resolution = 1.72 x 1.72 mm^2; slice thickness = 3 mm; b = 0, 1000 s/mm^2; number of slices = 40; acquisition time 8 minutes.

Dynamic Susceptibility Contrast-Perfusion Weighted Imaging

For axial DSC- PWI MR, a bolus of gadobenate dimeglumine (Multi-Hance; Bracco Diagnostics, Princeton, New Jersey) was injected with a preloading dose of 0.07 mmol/kg, to reduce the effect of contrast agent leakage on CBV measurements. A T2*-weighted gradient-echo EPI was used during the second 0.07 mmol /kg bolus of contrast agent for the DSC- PWI MR. The injection rate was 5 ml/s for all patients and was immediately followed by a flush of saline (total of 20 ml at the same rate). The sequence parameters were as follows: TR/TE = 2000/45 ms; FOV = 22 x 22 cm^2; matrix size = 128 x 128; in-plane resolution = 1.72 x 1.72 mm^2; slice thickness = 3 mm; BW = 1346 Hz/pixel; flip angle = 90°; EPI factor = 128; echo spacing = 0.83; acquisition time 3 minute and 10 seconds. Forty-five sequential measurements were acquired for each section. After the preloading dose of the contrast agent, routine sequences were also obtained, including axial T1-weighted 3D MPRAGE postcontrast (TR/TE/TI 1760/3.1/950 ms; 192 x 256 matrix size; 1-mm section thickness; acquisition time 3 minutes and

10 seconds) and axial FLAIR (TR/TE/TI 9420/141/2500 ms; 3-mm section thickness; acquisition time 3 minutes and 10 seconds).

Image Processing and Data Analysis

The motion and eddy current correction modules were applied to raw DTI data using in-house developed software (IDL; ITT Visual Information Solutions, Boulder, Colorado). Pixel-wise MD, FA, CL, CP, and spherical coefficient (CS) maps were computed by using the methods described earlier.[34,35] Leakage-corrected CBV maps were generated by performing gamma-variate curve fitting from DSC-PWI MR data using NordicICE software (NordicNeuroLab, Bergen, Norway).

The DTI derived maps, CBV maps, and T2-FLAIR images were resliced and co-registered to contrast-enhanced T1-weighted images. A semiautomatic approach was used to segment the contrast-enhancing regions of the dominant metastatic lesion by using a signal intensity-based thresholding method as defined previously.[34,35]

Tissue-Based Analysis

Representative histologic sections stained with hematoxylin-eosin and Masson's Trichrome were used to assess the stromal component (desmoplastic reaction) within the tumor by a board-certified neuropathologist (A.N.V.). The staining procedure for Masson's Trichrome included: slides were deparaffinized and hydrated, thereafter placed in Bouin's fixative for 1 hour in 60˚ C oven, washed in running tap water for 5 minutes, rinsed in deionized water, and stained in Weigert's Iron Hematoxylin for 10 minutes. Subsequently, slides were washed in running tap water for 10 minutes, rinsed in deionized water, stained in Beibrich Scarlet- Acid Fuchsin

solution for 15 minutes, and rinsed in deionized water, stained in Phosphotungstic acid for 2 minutes. Finally, the slides were stained in Aniline Blue solution for 1 to 5 minutes, rinsed in 1% acetic acid, dehydrated and coverslipped. The amount of tumor stroma was qualitatively assessed as low (scant to little), moderate, and high (stroma comprising a noticeable proportion of the overall tumor volume).

Final Data and Statistical Analysis

DTI metrics and DSC-PWI MR -derived CBV values were quantified from enhancing areas of dominant metastasis segmented semi-automatically, as described above. We used continuous values and various breakdowns in terms of coefficients (Q10, Q25, Q50, Q75, and Q90) for each parameter and percentiles (25th, 50th, and 75th percentile) to separate the patients into two risk groups (short and long-term survivors) in a univariate analysis. The best combination for each parameter from preliminary results was as follows, MD: the lower 10th percentile MD values (Q10) reported as minimum MD (MD_{min}) and subsequently separating the risk groups above and below the median (50th percentile) of the MD_{min}. FA/CL/CP/CS: the lower 25th percentile FA/CL/CP/CS values (Q25) and subsequently separated the risk groups above and below the first quartile (25th percentile) of the FA/CL/CP/CS Q25. rCBV: the top 90th percentile rCBV values (Q90) reported as $rCBV_{max}$ and subsequently separated the risk groups above and below the third quartile (75th percentile) of the $rCBV_{max}$. Kaplan-Meier survival curve plots and log-rank tests were used to compare the survival rates using the aforementioned imaging parameters (MD_{min}, FA Q25, CL Q25, CP Q25, CS Q25, and $rCBV_{max}$), as well as clinical variables (number of brain metastasis and site of primary tumor), and clinical scoring systems (GPA and RPA classes) as stratification factors. Subsequently, clinical and imaging variables that demonstrated significant predictive values and trends towards significance from univariate

survival analyses were incorporated into multivariate survival analysis using the Cox regression hazard model with backward conditional method. A probabilistic (p) value of less than 0.05 was considered significant. All statistical analyses were performed using a statistical package, SPSS for Windows (v. 18.0; Chicago, IL).

Additionally, a correlative histopathologic analysis was performed in a subset of patients on the opposite ends of the spectrum of DTI metrics and DSC-PWI MR derived $rCBV_{max}$. The DTI metrics were used as a surrogate marker of tumor cellularity and microarchitectural organization[13] and $rCBV_{max}$ for tumor angiogenesis and neovascularization.[27] Group 1 (n=6; Supplementary table 1: patients 12, 31, 66, 84, 87, and 94) was selected to represent the best combination of the lowest values of MD_{min} (impaired mobility of water; high cellularity) and the highest values of FA Q25 and CP Q25 (increased anisotropy; high organization of the tumor microarchitecture), and the lowest values of $rCBV_{max}$ (reduced angiogenesis; poor vascularity). Group 2 (n=4, Supplementary table 1: patients 13, 34, 77, and 81) was selected to have the best combination of the highest values of MD_{min} (facilitated mobility of water; low cellularity) and the lowest values of FA Q25 and CP Q25 (decreased anisotropy; poor organization of the tumor microarchitecture), and the highest values of $rCBV_{max}$ (elevated angiogenesis; increased vascularity). Of note, similar to the main cohort, this subcohort of patients also had metastatic tumors from a variety of primary sites (six lung adenocarcinomas, one breast adenocarcinoma, one colorectal adenocarcinoma, one high-grade neuroendocrine carcinoma of lung origin, and one sarcoma of lung origin).

Results

Patient and tumor characteristics Survival analysis

The Median KPS score was 80, and the median overall survival (mOS) for all patients was 301 days. In univariate analysis, survival differences by GPA class was significant (log-rank p<0.001. Class 1: 339.35 +/-128.79 days; Class 2: 682.64+/-100.49 days; Class 3: 1519.86 days; and Class 4: 1553.67 +/-425.63 days) and also for RPA class (log-rank p<0.001. Class 1: 1533.13 +/- 238.61 days; Class 2: 505.25 +/-72.71 days; Class 3: 123.75 +/-30.09 days), indicating a valid cohort. The mOS using tumor primary site (lung, breast, melanoma, kidney, colon, or other) was not significantly different (log-rank p>0.05), and the number of brain metastasis showed a trend towards significance (log-rank p=0.09), as independent predictors in univariate analysis.

Determination of long and short-term survivors using MRI data

Kaplan-Meier analyses revealed significant differences in mOS for MD_{min} (log-rank p<0.05), FA Q25 (log-rank p<0.01), CL Q25 (log-rank p<0.05), and CP Q25 (log-rank p<0.01), and trend towards significance for $rCBV_{max}$ (log-rank p=0.07). However, CS Q25 (log-rank p>0.05) did not predict survival (Figures 1 and 2 and Table 1).

Determination of the best predictive survival model

When statistically significant imaging and clinical independent prognostication parameters (MD_{min}, FA Q25, CL Q25, CP Q25, RPA, and GPA) and parameters with trends towards significance, such as $rCBV_{max}$ (log-rank p=0.07) and number of metastatic brain lesions (log-rank p=0.09), from univariate analyses were incorporated into Cox proportion hazard regression test, the best predictive survival model was obtained, which consisted of a combination of MD_{min}

(p=0.05), $rCBV_{max}$ (p<0.05), RPA (p<0.0001), and number of brain metastasis (p=0.07) in determining the OS.

Tissue-Based Analysis

Metastatic tumors showed an overall higher interstitial connective tissue (stromal component) in group 1 (n=6, mOS 83.33 +/-12.41 days) as compared to group 2 (n=4, mOS 1858.00 +/-707.81 days). The lowest values of MD_{min} and $rCBV_{max,}$ along with the highest values of FA Q25 and CP Q25 (group 1) significantly correlated with elevated stromal content and worse mOS (Figure 3). On the other hand, the highest values of MD_{min} and $rCBV_{max,}$ along with the lowest values of FA Q25 and CP Q25 (group 2) correlated with lower stromal content and better mOS (Figure 4). A quantitative measurement of the stromal component was not performed due to large variability across the slides. Thus, a qualitative assessment of low, moderate and high component was used instead. Assessment of the stromal component was facilitated by Masson's Trichrome stained sections (blue staining). These findings were consistent within the two groups regardless of tumor site of primary origin.

Discussion

The prognostic value of ADC is well-known for extracranial cancers in predicting survival, response to therapy, and even propensity to form brain metastasis.[36,37] Primary CNS tumors with low ADC values have also been associated with worse outcomes.[38–40] Recently, ADC incorporated with standard clinical parameters has shown to improve the prediction of overall survival in patients with surgically resected brain metastasis.[14] In this study, the MD_{min}, FA Q25, CL Q25, CP 25, and CBV_{max} as independent measures separated risk groups in short and long-term survivors, and in a multivariate analysis, the combination of MD_{min}, $rCBV_{max}$, RPA, and the

number of brain metastasis was the best predictive survival model, reinforcing the importance of MD_{min} and $rCBV_{max}$ as imaging parameters to predict OS and a possible confounding effect of RPA and the number of metastatic lesions. In addition, we demonstrated a correlation between the amount of desmoplastic reaction and mOS, substantiating the DTI metrics and $rCBV_{max}$ values.

The correlation of DTI-derived parameters and perfusion with patient outcomes has not been investigated in treatment naïve brain metastasis. However, a few studies reported the importance of ADC values in predicting survival in preoperative brain metastasis.[41,42] These studies reported aggressive tumor behavior in patients with low ADC values. In accordance with these studies, we also observed lower mOS in patients with MD_{min} below the median (similar physiological significance of ADC), and the MD_{min} remained statistically significant in multivariate analysis, supporting its prognostication value. However, other studies,[17–19] including from our group,[20] have demonstrated that the application of more gradient directions (DTI) can provide further tissue characterization and potentially be utilized for prognostication. We, therefore, evaluated several DTI parameters to noninvasively assess the tumor microarchitecture, demonstrating poor mOS in patients with low MD_{min} (impaired mobility of water) and high FA Q25, CL Q25, and CP 25 values (increased anisotropy). In other words, patients with high cellularity and organization of the tumor microarchitecture comprised short-term survivors. On the other hand, patients with high MD_{min} (facilitated mobility of water) and low FA Q25, CL Q25, and CP 25 values (decreased anisotropy), that is, low cellularity and disorganization of the tumor microarchitecture, were represented by long-term survivors.

Histopathologic studies have identified dense stromal matrix in primary tumors characterized by increased collagen fibril stiffness and anisotropy, described as a desmoplastic reaction, corroborating tumor growth.[43,44] In preoperative brain metastasis, Berghoff *et al.* 2013[42] reported a significant correlation of prominent interstitial fibrosis with the semiquantitative DWI signal intensity, resembling the impaired mobility of water molecules in the intercellular space. By extending the quantitative assessment of multiple DTI parameters, we demonstrated higher stromal component in patients with overall worse survival prognosis, represented by the lowest MD_{min} values and the highest values of FA Q25 and CP Q25. In contrast, patients with the highest MD_{min} values and the lowest FA Q25 and CP Q25 values presented with low cellular stromal component and had better long-term survival. These results from analyzed DTI metrics may reflect the tumor microarchitecture density and organization, reinforcing the importance of the interstitial space in the pathobiology of brain metastasis and the potential of quantitative DTI metrics to indirectly evaluate histopathological features.

The efficacy of chemoradiation therapy relies on the effective delivery of therapeutic agents and oxygen to the tumor cells. However, delivery of the drug and oxygen is often impeded by abnormal blood vessels and the presence of tumor hypoxia.[45] Using MRI-based perfusion parameters such as vascular transfer constant ($K^{trans,}$ a measure of tumor blood flow and vascular permeability), several previous studies[46–49] have reported that patients with extracranial cancers exhibiting elevated pretreatment K^{trans} harbor prolonged OS. In the present study, $rCBV_{max}$ was found to be a significant predictor in the determination of OS from Cox regression analysis, and brain metastasis patients with higher pretreatment $rCBV_{max}$ had longer mOS. Our results and those of earlier published reports support the notion that tumors with relatively higher blood flow/volume are associated with increased oxygenation levels resulting in better access to

chemotherapeutic drugs and radiosensitivity and thereby associated with improved survival outcomes.

The dense stromal matrix has also been correlated with pancreatic ductal adenocarcinoma with deficient vasculature limiting the delivery of chemotherapy and resulting in resistance to systemic therapies.[50] Therapeutic targeting of stromal cells increases intratumoral perfusion and enhances therapeutic delivery. In the current study, the group of patients with the lowest values of $rCBV_{max}$ (reduced tumor angiogenesis) showed higher stromal component and dismal survival rates. According to a prior histopathological study,[27] small peritumoral edema around brain metastasis was correlated with low microvascular density and neoangiogenic vascularization and was more likely to show brain-invasive growth than tumors with large edema. Therefore, rCBV as a measure of angiogenic activity may indirectly reflect tumor infiltration and predict OS. In a prior histopathological study, low neo-angiogenic activity in brain metastases has been associated with worse prognostic factor reflecting tumor infiltration.[27]

There is a growing body of evidence supporting that advanced MRI techniques could potentially be integrated into the widely validated prognostic models for brain metastases patients,[14] such as RPA or GPA scores, which can be improved with quantitative imaging metrics assessing the metabolic and physiologic information of the tumor. Our results suggest that the incorporation of $rCBV_{max}$ and MD_{min} DTI metrics could further enhance these prognostic markers, potentially contributing to therapeutic decision-making. For example, in future, brain metastases patients with a good prognosis can be offered more aggressive treatments, whereas, in patients with poor prognosis, optimal treatment focused on quality of life would be deemed more appropriate.

Despite promising findings, our study was also associated with certain limitations, including the retrospective study design. In addition, histological correlation was only performed on a limited sample size. Furthermore, our data is from a single institution and could benefit from validation in a multi-institutional cohort, preferably in a larger prospective study., perhaps investigating further directional diffusivity metrics, such as axial diffusivity (AD) and radial diffusivity (RD), which can potentially enhance the quantitate analysis.

Conclusion

In conclusion, we reported the prognostic value of DTI metrics and $rCBV_{max}$ in segregating long and short-term survivors with brain metastasis and their correlation with tissue-based stromal features. Additionally, we reinforced the importance of MD_{min} and $rCBV_{max}$ in a multivariate analysis. Further validation in larger prospective studies in a multi-institutional setting may substantiate the incorporation of advanced imaging techniques into established risk stratification models.

References

1. Soffietti R, Rudā R, Mutani R. Management of brain metastases. *J Neurol* 2002;249:1357–69.

2. Gavrilovic IT, Posner JB. Brain metastases: epidemiology and pathophysiology. *J Neurooncol* 2005;75:5–14.

3. Fox BD, Cheung VJ, Patel AJ, et al. Epidemiology of metastatic brain tumors. *Neurosurg Clin N Am* 2011;22:1–6, v.

4. Sperduto PW, Berkey B, Gaspar LE, et al. A new prognostic index and comparison to three other indices for patients with brain metastases: an analysis of 1,960 patients in the RTOG database. *Int J Radiat Oncol Biol Phys* 2008;70:510–4.

5. Gaspar L, Scott C, Rotman M, et al. Recursive partitioning analysis (RPA) of prognostic factors in three radiation therapy oncology group (RTOG) brain metastases trials. *International Journal of Radiation Oncology*Biology*Physics* 1997;37:745–51.

6. Sperduto PW, Kased N, Roberge D, et al. Summary report on the graded prognostic assessment: an accurate and facile diagnosis-specific tool to estimate survival for patients with brain metastases. *J Clin Oncol* 2012;30:419–25.

7. Yamamoto M, Sato Y, Serizawa T, et al. Subclassification of recursive partitioning analysis Class II patients with brain metastases treated radiosurgically. *Int J Radiat Oncol Biol Phys* 2012;83:1399–405.

8. Serizawa T, Higuchi Y, Nagano O, et al. Testing different brain metastasis grading systems in stereotactic radiosurgery: Radiation Therapy Oncology Group's RPA, SIR, BSBM, GPA, and modified RPA. *J Neurosurg* 2012;117 Suppl:31–7.

9. Barnholtz-Sloan JS, Yu C, Sloan AE, et al. A nomogram for individualized estimation of survival among patients with brain metastasis. *Neuro Oncol* 2012;14:910–8.

10. Viani GA, Bernardes da Silva LG, Stefano EJ. Prognostic Indexes for Brain Metastases: Which Is the Most Powerful? *International Journal of Radiation Oncology*Biology*Physics* 2012;83:e325–30.

11. Nieder C, Andratschke N, Grosu AL, et al. Recursive partitioning analysis (RPA) class does not predict survival in patients with four or more brain metastases. *European Journal of Cancer* 2001;37:S341.

12. Estabrook NC, Lutz ST, Johnson CS, et al. Does Graded Prognostic Assessment outperform Recursive Partitioning Analysis in patients with moderate prognosis brain metastases? *CNS Oncology* 2016;5:69–76.

13. Pope WB. Brain metastases: neuroimaging. *Handb Clin Neurol* 2018;149:89–112.

14. Zakaria R, Chen YJ, Hughes DM, et al. Does the application of diffusion weighted imaging improve the prediction of survival in patients with resected brain metastases? A retrospective multicenter study. *Cancer Imaging* 2020;20:16.

15. Alexander AL, Hasan K, Kindlmann G, et al. A geometric analysis of diffusion tensor measurements of the human brain. *Magn Reson Med* 2000;44:283–91.

16. Westin C-F, Maier SE, Mamata H, et al. Processing and visualization for diffusion tensor MRI. *Med Image Anal* 2002;6:93–108.

17. Calli C, Kitis O, Yunten N, et al. Perfusion and diffusion MR imaging in enhancing malignant cerebral tumors. *Eur J Radiol* 2006;58:394–403.

18. Tsuchiya K, Fujikawa A, Nakajima M, et al. Differentiation between solitary brain metastasis and high-grade glioma by diffusion tensor imaging. *Br J Radiol* 2005;78:533–7.

19. Yamasaki F, Kurisu K, Satoh K, et al. Apparent diffusion coefficient of human brain tumors at MR imaging. *Radiology* 2005;235:985–91.

20. Wang S, Kim S, Chawla S, et al. Differentiation between Glioblastomas, Solitary Brain Metastases, and Primary Cerebral Lymphomas Using Diffusion Tensor and Dynamic Susceptibility Contrast-Enhanced MR Imaging. *American Journal of Neuroradiology* 2011;32:507–14.

21. Mohan S, Wang S, Coban G, et al. Detection of occult neoplastic infiltration in the corpus callosum and prediction of overall survival in patients with glioblastoma using diffusion tensor imaging. *Eur J Radiol* 2019;112:106–11.

22. Lacerda S, Law M. Magnetic resonance perfusion and permeability imaging in brain tumors. *Neuroimaging Clin N Am* 2009;19:527–57.

23. Thompson G, Mills SJ, Stivaros SM, et al. Imaging of brain tumors: perfusion/permeability. *Neuroimaging Clin N Am* 2010;20:337–53.

24. Romano A, Pasquini L, Di Napoli A, et al. Prediction of survival in patients affected by glioblastoma: histogram analysis of perfusion MRI. *J Neurooncol* 2018;139:455–60.

25. Law M, Young RJ, Babb JS, et al. Gliomas: Predicting Time to Progression or Survival with Cerebral Blood Volume Measurements at Dynamic Susceptibility-weighted Contrast-enhanced Perfusion MR Imaging. *Radiology* 2008;247:490–8.

26. Bag AK, Cezayirli PC, Davenport JJ, et al. Survival analysis in patients with newly diagnosed primary glioblastoma multiforme using pre- and post-treatment peritumoral perfusion imaging parameters. *J Neurooncol* 2014;120:361–70.

27. Spanberger T, Berghoff AS, Dinhof C, et al. Extent of peritumoral brain edema correlates with prognosis, tumoral growth pattern, HIF1a expression and angiogenic activity in patients with single brain metastases. *Clin Exp Metastasis* 2013;30:357–68.

28. Essig M, Waschkies M, Wenz F, et al. Assessment of Brain Metastases with Dynamic Susceptibility-weighted Contrast-enhanced MR Imaging: Initial Results. *Radiology* 2003;228:193–9.

29. Zakaria R, Das K, Bhojak M, et al. The role of magnetic resonance imaging in the management of brain metastases: diagnosis to prognosis. *Cancer Imaging* 2014;14:8.

30. Brancato V, Nuzzo S, Tramontano L, et al. Predicting Survival in Glioblastoma Patients Using Diffusion MR Imaging Metrics—A Systematic Review. *Cancers* 2020;12:2858.

31. Park JE, Kim HS, Jo Y, et al. Radiomics prognostication model in glioblastoma using diffusion- and perfusion-weighted MRI. *Scientific Reports* 2020;10.

32. Petrova L, Korfiatis P, Petr O, et al. Cerebral blood volume and apparent diffusion coefficient - Valuable predictors of non-response to bevacizumab treatment in patients with recurrent glioblastoma. *J Neurol Sci* 2019;405:116433.

33. Puig J, Sánchez-González J, Blasco G, et al. Intravoxel Incoherent Motion Metrics as Potential Biomarkers for Survival in Glioblastoma. *PLoS One* 2016;11:e0158887.

34. Wang S, Kim S, Chawla S, et al. Differentiation between glioblastomas and solitary brain metastases using diffusion tensor imaging. *Neuroimage* 2009;44:653–60.

35. Chawla S, Wang S, Mohan S, et al. Differentiation of brain infection from necrotic glioblastoma using combined analysis of diffusion and perfusion MRI. *J Magn Reson Imaging* 2019;49:184–94.

36. Nakajo M, Kajiya Y, Kaneko T, et al. FDG PET/CT and diffusion-weighted imaging for breast cancer: prognostic value of maximum standardized uptake values and apparent diffusion coefficient values of the primary lesion. *European Journal of Nuclear Medicine and Molecular Imaging* 2010;37:2011–20.

37. Ohno Y, Koyama H, Yoshikawa T, et al. Diffusion-Weighted MRI Versus 18F-FDG PET/CT: Performance as Predictors of Tumor Treatment Response and Patient Survival in Patients With Non–Small Cell Lung Cancer Receiving Chemoradiotherapy. *American Journal of Roentgenology* 2012;198:75–82.

38. Barajas RF Jr, Rubenstein JL, Chang JS, et al. Diffusion-weighted MR imaging derived apparent diffusion coefficient is predictive of clinical outcome in primary central nervous system lymphoma. *AJNR Am J Neuroradiol* 2010;31:60–6.

39. Wu C-C, Jain R, Radmanesh A, et al. Predicting Genotype and Survival in Glioma Using Standard Clinical MR Imaging Apparent Diffusion Coefficient Images: A Pilot Study from The Cancer Genome Atlas. *AJNR Am J Neuroradiol* 2018;39:1814–20.

40. Kim BS, Kim ST, Kim JH, et al. Apparent Diffusion Coefficient as a Predictive Biomarker for Survival in Patients with Treatment-Naive Glioblastoma Using Quantitative Multiparametric Magnetic Resonance Profiling. *World Neurosurgery* 2019;122:e812–20.

41. Zakaria R, Das K, Radon M, et al. Diffusion-weighted MRI characteristics of the cerebral metastasis to brain boundary predicts patient outcomes. *BMC Medical Imaging* 2014;14.

42. Berghoff AS, Spanberger T, Ilhan-Mutlu A, et al. Preoperative diffusion-weighted imaging of single brain metastases correlates with patient survival times. *PLoS One* 2013;8:e55464.

43. Koontongkaew S. The tumor microenvironment contribution to development, growth, invasion and metastasis of head and neck squamous cell carcinomas. *J Cancer* 2013;4:66–83.

44. Pham TT, Stait-Gardner T, Lee CS, et al. Correlation of ultra-high field MRI with histopathology for evaluation of rectal cancer heterogeneity. *Sci Rep* 2019;9:9311.

45. Vaupel P, Kallinowski F, Okunieff P. Blood flow, oxygen and nutrient supply, and metabolic microenvironment of human tumors: a review. *Cancer Res* 1989;49:6449–65.

46. Chawla S, Loevner LA, Kim SG, et al. Dynamic Contrast-Enhanced MRI-Derived Intracellular Water Lifetime (τ): A Prognostic Marker for Patients with Head and Neck Squamous Cell Carcinomas. *AJNR Am J Neuroradiol* 2018;39:138–44.

47. Chawla S, Kim S, Loevner LA, et al. Prediction of disease-free survival in patients with squamous cell carcinomas of the head and neck using dynamic contrast-enhanced MR imaging. *AJNR Am J Neuroradiol* 2011;32:778–84.

48. Lichtor T. *Molecular Considerations and Evolving Surgical Management Issues in the Treatment of Patients with a Brain Tumor*. BoD – Books on Demand; 2015.

49. Ohno Y, Nogami M, Higashino T, et al. Prognostic value of dynamic MR imaging for non-small-cell lung cancer patients after chemoradiotherapy. *J Magn Reson Imaging* 2005;21:775–83.

50. Neesse A, Michl P, Frese KK, et al. Stromal biology and therapy in pancreatic cancer. *Gut* 2011;60:861–8.

Figures' legends:

Figure 1: Kaplan Meier curves showing significantly higher overall survival (log-rank p=0.013) in patients with MD_{min} above 50th percentile, significantly higher overall survival (log-rank p=0.009) in patients with FA Q25 below 25th percentile, and significantly higher overall survival (log-rank p=0.009) in patients with CP Q25 below 25th percentile.

Figure 2: Kaplan Meier curves showing non-significant differences in overall survival in terms of CS Q25 (log-rank p=0.384) and $rCBV_{max}$ (log-rank p=0.073).

Figure 3: 55-year-old female with metastatic adenocarcinoma of colorectal origin, prior to any treatment for brain metastasis, presenting with mOS of 62 days. (A) Contrast-enhanced T1-weighted image shows a heterogeneous enhancing lesion in the left inferior frontal lobe. (B) FLAIR images demonstrate surrounding vasogenic edema. (C) Decreased ADC (ADC_{min} = 0,000692) and (D) very high FA (FA Q25 = 0,12) values from the enhancing part. (E) DSC-PWI MRI with low rCBV from the enhancing region of the tumor ($rCBV_{max}$ = 6.28; white arrows in E). (F) and (G) Pathology from surgical resection demonstrates high stromal component (blue staining, black arrows in G). H&E stain (F) and Masson's trichrome stain (G). Histological photos were taken at 100x magnification.

Figure 4: 45-year-old female with metastatic adenocarcinoma of breast, prior to any treatment for brain metastasis, presenting with mOS of 2859 days. (A) Contrast-enhanced T1-weighted image shows a ring enhancing lesion delimitating a central area of necrosis in the left temporal lobe. (B) FLAIR images demonstrate surrounding vasogenic edema. (C) Increased ADC (ADC_{min} = 0,000905) and (D) very low FA (FA Q25 = 0,057) values from the enhancing part. (E) DSC- PWI MRI with elevated rCBV from the enhancing region of the tumor ($rCBV_{max}$ = 8.64, white arrows in E). (F) and (G) Pathology from surgical resection demonstrates a smaller

stromal component (blue staining, white arrows in G). H&E stain (F) and Masson's trichrome stain (G). Histological photos were taken at 100x magnification.

Table 1:

Title: Determination of long and short-term survivors using MRI data.

Supplementary Table1:

Title: Demographic, clinical, and diffusion and perfusion MRI-derived parameters.

Abbreviations: BM = brain metastasis; **KPS** = Karnofsky performance status; **GPA:** graded prognostic assessment. **RPA** = recursive portioning analysis; OS: overall survival. $\mathbf{MD_{min}}$: minimum mean diffusivity. **FA** = fractional anisotropy; **CP** = planar coefficien; **CS** = spherical coefficient. $\mathbf{rCBV_{max}}$ = maximum relative cerebral blood volume.

Figure 1

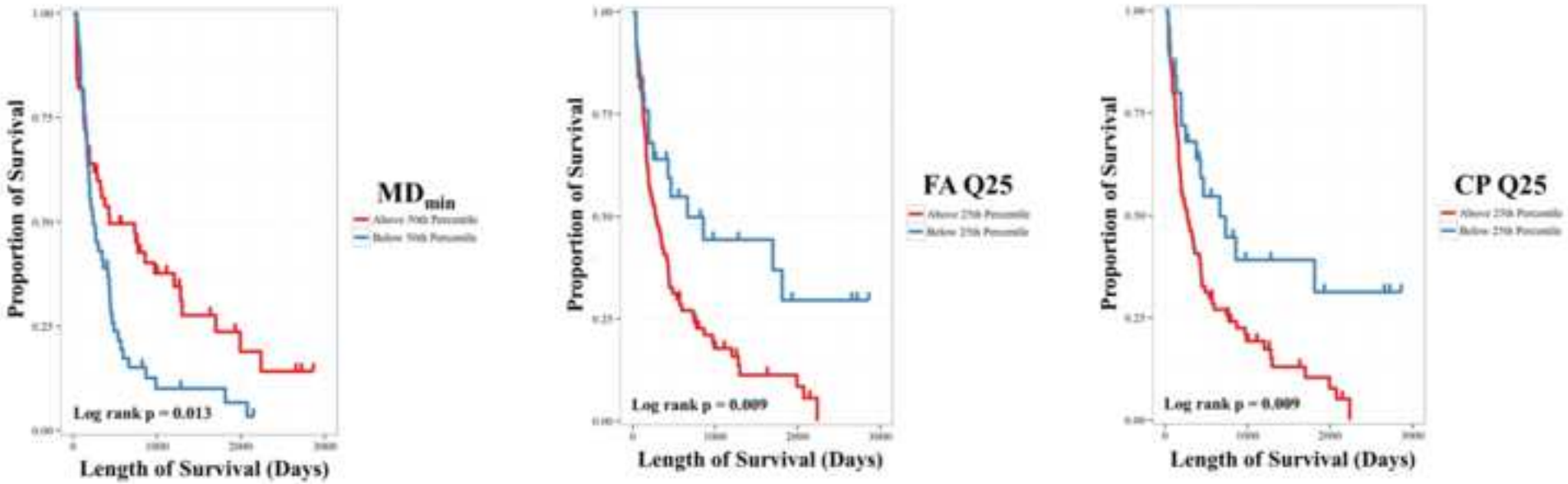

Figure 2

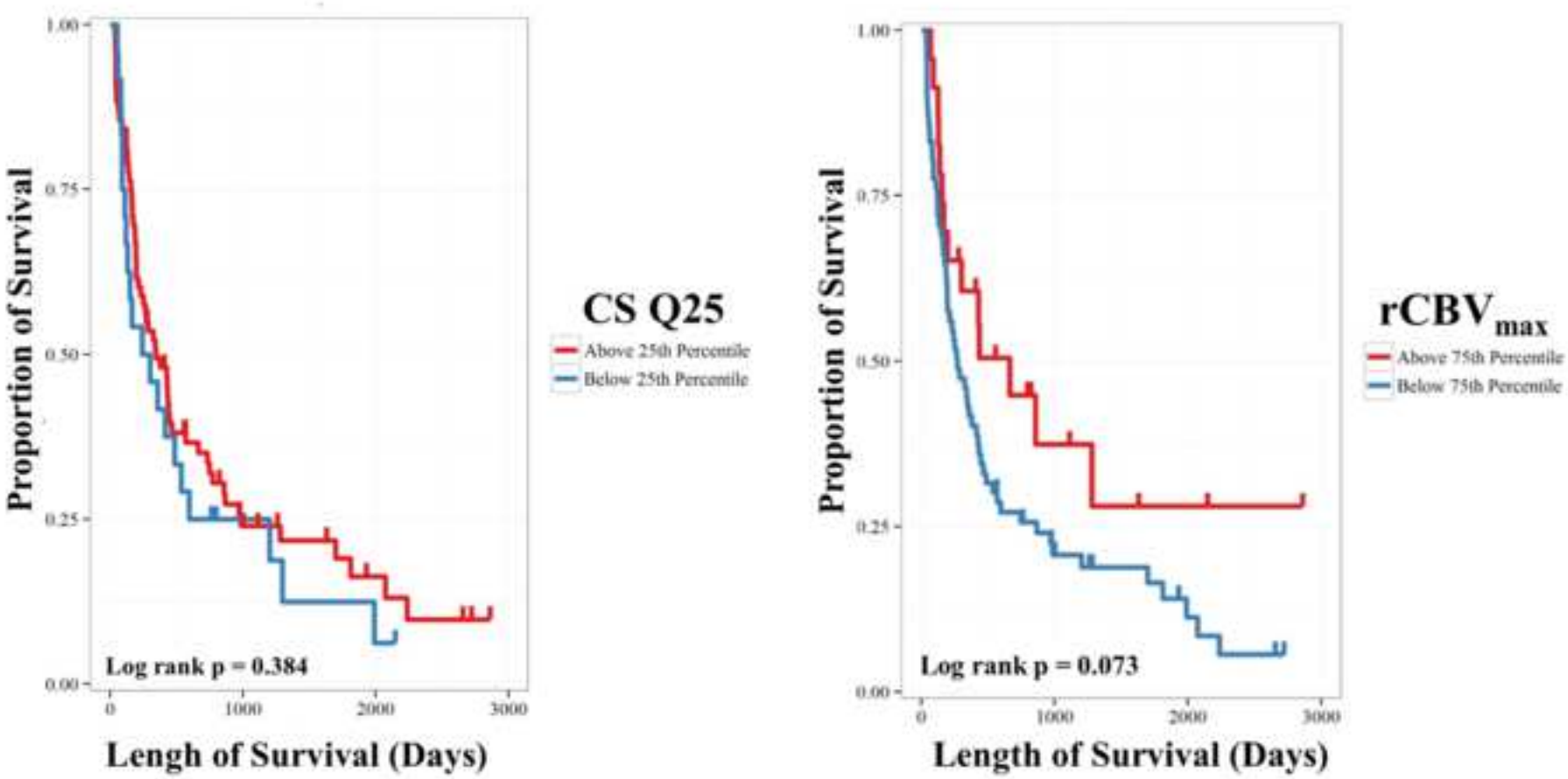

Figure 3

Click here to access/download;Figure;Figure 3_BJR.tiff

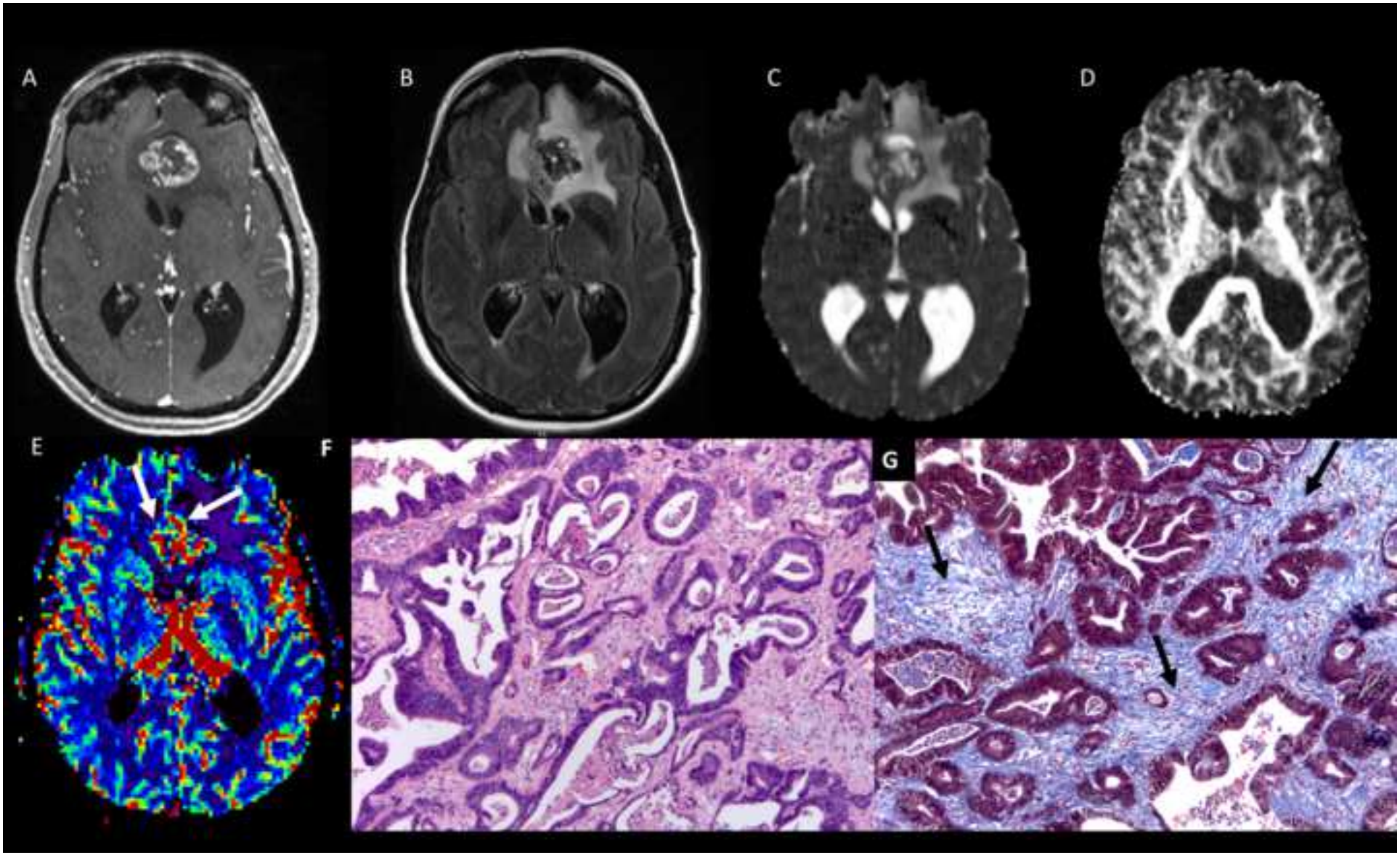

Figure 4

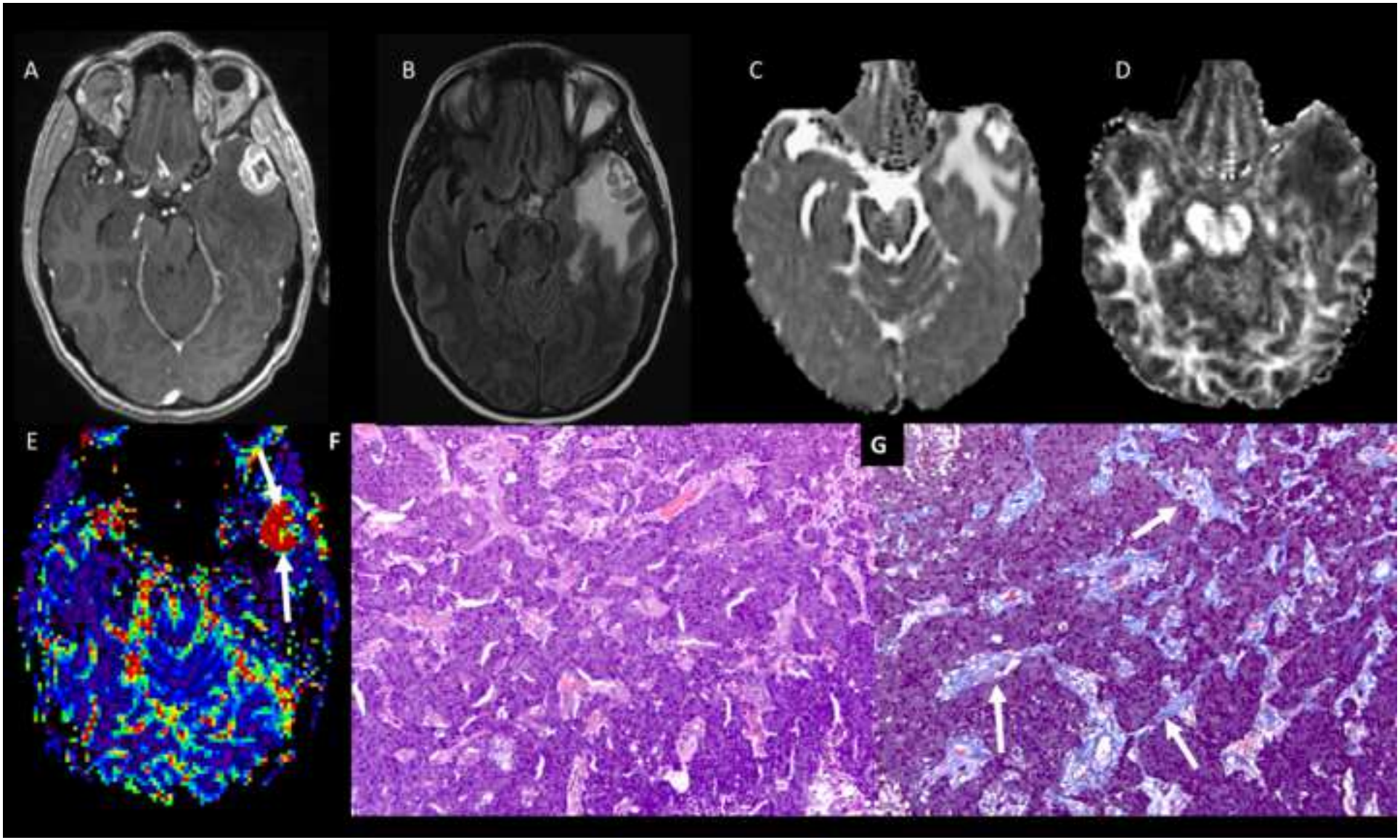

Table

Table 1. Determination of long and short-term survivors using MRI data

Coefficients	**Percentiles**	**mOS**	**log-rank p**
MD_{min}	Below the 50th percentile	470.81+/-82.44	<0.05
	Above the 50th percentile	983.44 +/-153.19	
FA Q25	Below the 25th percentile	1269.92 +/- 249.96	<0.01
	Above the 25th percentile	565.073 +/- 78.75	
CL Q25	Below the 25th percentile	1162.31 +/-240.35	<0.05
	Above 25th percentile	622.832+/-92.68	
CP Q25	Below the 25th percentile	1253.06 +/-252.02	<0.01
	Above 25th percentile	571.86+/-79.64	
CS Q25	Below the 25th percentile	584.62 +/-140.18	>0.05
	Above 25th percentile	785.69+/-111.94	
$rCBV_{max}$	Below the 75th percentile	853.19+/-98.71	0.07
	Above the 75th percentile	1126.57+/-268.98	

Abbreviations:

CL- linear coefficient; CP- planar coefficient; CS- spherical coefficient; FA-fractional anisotropy; MDmin – minimum mean diffusivity; mOS – median overall survival; rCBVmax- maximum relative cerebral blood volume